

Collective infectivity of the pandemic over time and association with vaccine coverage and economic development

Nick James^a, Max Menzies^b

^a*School of Mathematics and Statistics, University of Melbourne, Victoria, Australia*

^b*Beijing Institute of Mathematical Sciences and Applications, Tsinghua University, Beijing, China*

Abstract

This paper uses new and existing methods to study the evolution of COVID-19's global infectivity, the rollout of the vaccine, and its association with reduced cases and deaths. We begin with a time-varying analysis of the collective nature of infectivity, where we evaluate the eigenspectrum of reproductive rate time series on a country-by-country basis. We then study the topology of this eigenspectrum, measuring the deviation between all points in time, and introduce a graph-theoretic methodology to reveal a clear partition in global infectivity dynamics. We then compare different countries' vaccine rollouts with economic indicators such as their GDP and HDI. We investigate time-varying consistency and determine points in time where there is the greatest discrepancy between the most and least economically advanced countries. Finally, we use two supervised learning models to determine the feature importance and association between time, vaccine proliferation, cases and deaths. We demonstrate that the vaccine had a significant association with reduced COVID-19 deaths, but no association with reduced case counts.

Keywords: COVID-19 infectivity, Time series analysis, Graph theory, Nonlinear dynamics

1. Introduction

Throughout the course of the COVID-19 pandemic, the focus of research on the virus and its infectivity has continued to shift. Initial research explored risk factors, in-patient mortality rates and recovery times [1, 2], with a substantial of early analysis performed in China [3–7]. Since then, medical researchers have thoroughly investigated and discovered new treatments [8–11], followed by the invention of several vaccines [12–14]. The aforementioned clinical research has

Email addresses: nick.james@unimelb.edu.au (Nick James),
max.menzies@alumni.harvard.edu (Max Menzies)

broadened into much wider research into all the public health consequences of the pandemic, including mental health [15, 16] and investigations into health care systems [17].

Beginning slightly later than the medical research, a substantial body of research in the mathematical biology, applied mathematics, and nonlinear dynamics communities has emerged for analysing and forecasting the spread of the virus. The analytic approaches used have been broad and have continued to grow. First, many models based on classical mathematical models, such as the Susceptible–Infected–Recovered (SIR) model and the reproductive ratio R_0 , have been proposed and systematically collated by researchers [18, 19]. These have been utilised for numerous purposes, including diagnosis and prognosis of COVID-19 patients, studies of the efficacy of medications, and vaccine development. Next, nonlinear dynamics researchers have proposed many sophisticated extensions to the classical predictive SIR model, including analytic techniques to find explicit solutions [20, 21], modifications to the model with additional variables [22–27], incorporation of Hamiltonian dynamics [28] or network models [29], and a closer analysis of uncertainty in the SIR equations [30]. Other mathematical approaches to analysis and prediction include power-law models [31–33], forecasting models [34], fractal approaches [35–37], neural networks [38], methods from Bayesian statistics [39, 40], distance analysis [41], network models [42–45], analyses of the dynamics of transmission and contact [46, 47], clustering [48–50] and many others [51–55]. This community of researchers is inherently interdisciplinary, so have frequently studied other impacts of COVID-19 outside epidemiology, such as its effect on financial and cryptocurrency markets [56–69]. Finally, numerous more recent articles have been devoted to understanding the spatial components of the virus’ spread, in numerous countries [70–73].

In more recent times, the pandemic and its associated research have taken a different form. Most developed countries have essentially completed their vaccine rollout, and yet cases continue to exhibit new peaks throughout many different regions [74]. In addition, most countries have reduced their restrictions and opened their borders, meaning they are no longer isolated ecosystems. Thus, a new body of work has emerged with an emphasis on necessary collaboration between countries to mitigate ongoing risks of COVID-19 [75, 76]. Vaccines remain an integral part of that response, so ongoing research is necessary to determine their impact on cases and effectiveness [77]. While much of this is medical research [78–80], there remains an ongoing need for mathematical and nonlinear dynamics results to examine broader trends [81].

Our work is heavily inspired by the aforementioned trends in the recent literature, but we take a different approach. While existing work has discussed and called for further cooperation between countries to continue mitigating COVID-19 after the vaccine rollout, little mathematical work has examined collective trends in infectivity on a country-by-country basis, especially incorporating the interplay with the vaccine rollout. Nor are we aware of any research within the framework of time series analysis that studies collective behaviour of infectivity time series on a country-by-country basis. The authors have produced previous work analysing trends in cases and deaths on a country-by-country or

state-by-state basis [82], but have never analysed infectivity time series, collective correlation strength, or the relationship with vaccine doses.

Our paper is structured as follows. Section 2 summarises all the data we draw upon in this work. In Section 3, we study collective dynamics of various countries’ reproduction rate time series. We use methods of time series analysis typically used in financial and other applications [83–87]. In particular, we notice an abrupt increase in collective dynamics from approximately March/April 2021. In Section 4, we analyse this more closely with graph-theory-inspired methods, identifying a point in time that exhibits maximal separation in the eigenspectrum. In Section 5, we study the time-varying consistency between countries’ vaccine proliferation and their economic and human development. In Section 6, we implement two supervised learning algorithms to aid in our understanding of the relationship between the timing and progress of a country’s vaccine rollout and the associated impact on COVID-19 related cases and deaths. In Section 7, we conclude.

2. Data

All the data used in this paper are obtained from Our World in Data (<https://ourworldindata.org/coronavirus>). We select the $N = 50$ countries with the greatest total reported case counts as of June 2022 and consider four time series: reproductive rate R_0 , according to their method of estimation [88], confirmed case counts, reported death counts, and counts of fully vaccinated individuals. Our data spans a period of 1 April 2020 to 1 May 2022, in total $T = 761$ days.

3. Time-varying collective infectivity

Let $R_i(t)$ be the multivariate time series of daily reproductive rate (“ R_0 ”) values for countries listed alphabetically and indexed $i = 1, \dots, N, t = 1, \dots, T$. We begin by choosing a window of $\tau = 90$ days over which we compute correlations between rolling R_0 time series. This approach is inspired by analyses of correlations and distances between financial time series [89–95]. These are defined as follows: for $t = \tau, \dots, T$, define an $N \times N$ matrix $\Psi(t)$ by

$$\Psi_{ij}(t) = \frac{1}{\tau} \frac{\sum_{s=t-\tau+1}^t (R_i(s) - \langle R_i \rangle)(R_j(s) - \langle R_j \rangle)}{\left(\sum_{s=t-\tau+1}^t (R_i(s) - \langle R_i \rangle)^2 \right)^{1/2} \left(\sum_{s=t-\tau+1}^t (R_j(s) - \langle R_j \rangle)^2 \right)^{1/2}}, \quad (1)$$

$$i, j = 1, \dots, N, \quad (2)$$

where $\langle \cdot \rangle$ denotes the temporal average over the time window $[t - \tau + 1, t]$. We can gain additional understanding of this matrix by decomposing it as follows:

$$\Psi(t) = \frac{1}{\tau} \tilde{R} \tilde{R}^T. \quad (3)$$

In the equation (3) above, \tilde{R} is a $N \times \tau$ matrix of standardised R_0 values obtained by rescaling by the mean $\langle \cdot \rangle$ and standard deviation $\sigma(\cdot)$ over the interval $[t - \tau + 1, t]$, namely $\tilde{R}_i(s) = [R_i(s) - \langle R_i \rangle] / \sigma(R_i)$.

With this matrix decomposition, we may deduce that $\Psi(t)$ is a symmetric positive semi-definite matrix whose entries lie in $[-1, 1]$. It carries real and non-negative eigenvalues $\lambda_i(t)$ that we can reorder by $\lambda_1 \geq \lambda_2 \geq \dots \geq \lambda_N$. These convey the magnitude of different axes of variation within $\Psi(t)$. As all diagonal entries of Ψ coincide with 1, the trace of Ψ is equal to N . Thus, we may normalise the eigenvalues by defining $\tilde{\lambda}_i = \frac{\lambda_i}{\sum_{j=1}^N \lambda_j} = \frac{\lambda_i}{N}$. In particular, $\tilde{\lambda}_1(t)$ coincides with a normalised *operator norm* [96]:

$$\tilde{\lambda}_1(t) = \frac{1}{N} \|\Psi(t)\|_{op} = \frac{1}{N} \sup_{v \in \mathbb{R}^N - \{0\}} \frac{\|\Psi(t)v\|}{\|v\|}, \quad (4)$$

which gives a measure of the overall size of the matrix $\Psi(t)$ or the collective strength of correlations.

We display the function $\tilde{\lambda}_1(t)$ in Figure 1. This shows the evolution of the collective strength of correlations between reproductive rate time series during our window of analysis. The shape of the function tells an interesting story, with three key insights. First, there is significant variability in the range of collective behaviour of countries' infectivity, with the value of $\lambda_1(t)$ ranging from ~ 0.3 to ~ 0.6 . Second, there is clearly a sharp increase (translation upward) in global collective behaviours around March-April 2021. It is likely that this period corresponds to two key themes. This time period is broadly consistent with the onset of the delta variant, which was significantly more infectious than prior strains of COVID-19. Furthermore, many countries began lifting restrictions, with a larger proportion of their populations having been vaccinated. This likely led to a greater number of susceptible candidates transmitting COVID-19 to one another in various countries and hence greater collective uniformity and correlation strength between countries. The final notable insight is the significant increase in the oscillatory behaviour of the function beyond March-April 2021. There are at least 5 "waves" of collective infectivity in the latter part of our graph. This may be indicative of the "stop-start" nature of many countries' economic policies with regards to their gradual reopening, and the gradual evolution of the COVID-19 virus.

4. Graph-theoretic partition

In the above section, we highlight the marked change in collective homogeneity of infectivity (summarised by $\lambda_1(t)$ of rolling R_0 time series) around March/April

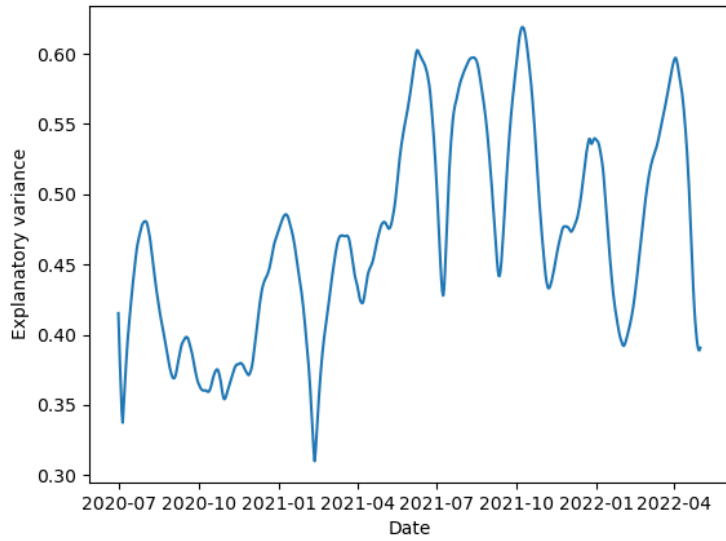


Figure 1: Trends in the normalised first eigenvalue $\tilde{\lambda}_1$, as defined and discussed in (4). Each indexed date summarises provides a measure of the collective strength of correlations between reproductive rate time series over the prior 90 days. We observe a sharp translation upward during the latter half of the period analysed. In addition, there is the emergence of wave-type behaviours in the strength of collective infectivity.

2021. In this section, we aim to elucidate and quantify this notable change point via a novel approach informed by graph theory. We further analyse the previous section's primary object of study, the time series $\tilde{\lambda}_1(t), t = \tau, \dots, T$. First, for $s, t = \tau, \dots, T$, we construct a distance that distinguishes between such values, $d(s, t) = |\tilde{\lambda}_1(s) - \tilde{\lambda}_1(t)|$. This produces a $(T - \tau + 1) \times (T - \tau + 1)$ distance matrix $D_{st} = d(s, t)$. For notational convenience, let $T_1 = T - \tau + 1$. We can also associate a corresponding $T_1 \times T_1$ *affinity matrix* defined by

$$A_{st} = 1 - \frac{D_{st}}{\max D}, s, t = \tau, \dots, T. \quad (5)$$

We define the primary change point in the time series $\tilde{\lambda}_1(t)$ as follows:

$$T_0 = \underset{p}{\operatorname{argmax}} f(p); \quad (6)$$

$$f(p) = \frac{1}{p(T_1 - p)} \sum_{s \leq p, t > p} D_{st}. \quad (7)$$

That is, T_0 is chosen to maximise the normalised distance (calculated from D) between times before and after T_0 .

This approach is inspired by graph theory and can be interpreted as follows. Let $G = (V, E)$ be a (weighted) graph with vertex set $V = \{\tau, \dots, T\}$ and edge set E where every two s, t are connected by an edge of weight $d(s, t)$. Then T_0 is chosen subject to two constraints:

- We wish to partition the vertex set into $V = V_1 \cup V_2$ such that V_1 and V_2 are disjoint and unbroken time intervals;
- subject to the above, we wish to find a *maximum cut* of the graph subject to its edge weighting.

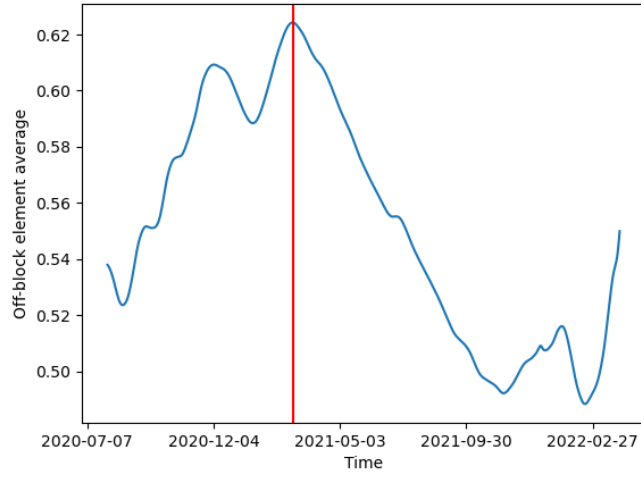
For the sake of robustness, we also present an alternative method to determine a primary change point. As an alternative approach, we define

$$S_0 = \underset{p}{\operatorname{argmax}} g(p); \quad (8)$$

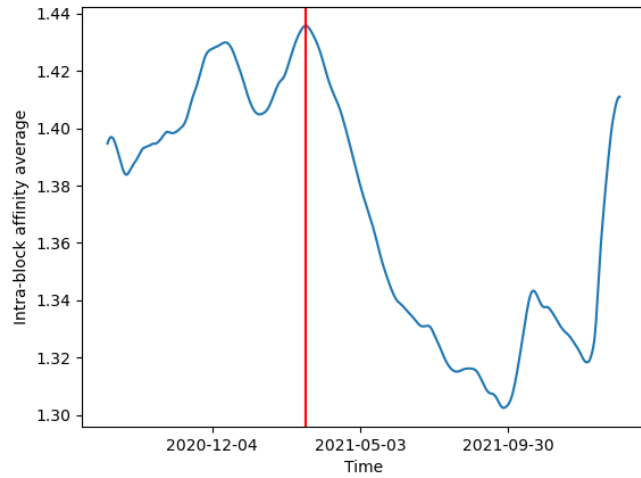
$$g(p) = \frac{1}{p^2} \sum_{s, t \leq p} A_{st} + \frac{1}{(T_1 - p)^2} \sum_{s, t > p} A_{st}. \quad (9)$$

Here S_0 is chosen to maximise the (normalised) collective affinity between times both before and after S_0 . This definition is also inspired by graph theory, but aims to find a *minimum cut* of the graph subject to an alternative edge weighting where every two s, t are connected by an edge of weight A_{st} , their affinity.

In Figure 2, we plot both the aforementioned functions $f(p)$ and $g(p)$ as well as their respective maxima, T_0 and S_0 , as defined above. The considerable similarity in the figures demonstrates the robustness of the method, and together they reveal the point in time corresponding to the most abrupt change in collective infectivity. The red vertical lines correspond to the points T_0 and S_0



(a)



(b)

Figure 2: Trends in the functions (a) $f(p)$, defined in (7), and (b) $g(p)$, defined in (9). These measure the normalised distance between and affinity among the values of the first eigenvalue corresponding to times before and after time p , respectively. Vertical red lines denote the respective maximal values, defined as T_0 and S_0 respectively, as in Section 4. The similarity of the observed maxima demonstrates the robustness of our methodologies to identify the cleanest separation in the evolution of $\tilde{\lambda}_1(t)$.

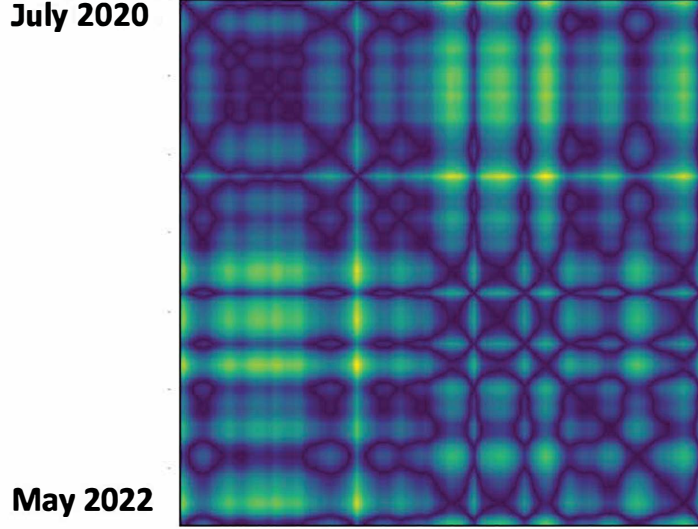


Figure 3: Heat map depicting values of $d(s, t)$ determining the distance between the normalised first eigenvalue $\tilde{\lambda}_1(t)$ at all points $t = \tau, \dots, T$. As each value of $\tilde{\lambda}_1(t)$ reflects behaviour over the previous 90 days, the figure begins with July 2020. Lighter values indicate greater values of $d(s, t)$.

in time that maximise the aforementioned separation in our graph's structure. This maximum corresponds to approximately March/April 2021, and reflects the sharp increase in collective behaviours during the second half of our period of analysis.

Figure 3 provides more visual detail regarding the distance $d(s, t) = |\tilde{\lambda}_1(s) - \tilde{\lambda}_1(t)|$. This figure displays all values of the distance for $s, t = \tau, \dots, T$. Such a heat map can reveal clear patterns in the distance between elements and offer the possibility of applying methods such as hierarchical clustering [97–100]. We also plot an alternative distance in Figure 4, defined by $d^{10}(s, t) = \sum_{k=1}^{10} |\tilde{\lambda}_k(s) - \tilde{\lambda}_k(t)|$, incorporating the first ten normalised eigenvalues. Figures 3 and 4 convey a similar story, with two sub-matrices exhibiting high self-similarity. Both figures are consistent with our finding in Figure 2, and suggest a clear break in the structure of the $d(s, t)$ matrix corresponding to March/April 2021. However, there are several subtle differences between Figure 3 and Figure 4 that are worth highlighting. First, Figure 3, which displays distances between $\tilde{\lambda}_1$ at various points in time, consists of a sharper distinction between the two sub-matrices. By contrast, Figure 4, which computes distances between the first ten normalised elements of the eigenspectrum $\tilde{\lambda}_1, \dots, \tilde{\lambda}_{10}$, displays a more diffuse transition between the two periods. The second key insight, which is highly consistent between Figures 3 and 4, is the interesting geometry displayed in the secondary sub-matrix. This feature reflects the periodic behaviour of the eigenspectrum

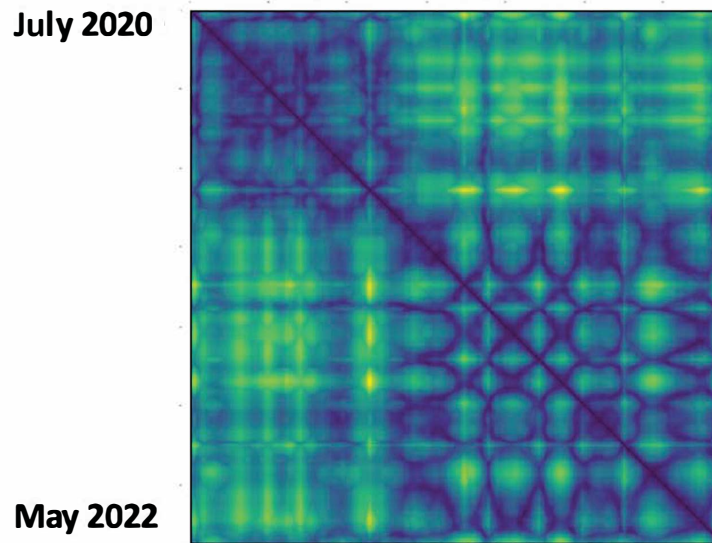


Figure 4: Heat map depicting values of $d^{10}(s, t)$ determining the distance between the normalised first ten eigenvalues $\lambda_i(t)$, $i = 1, \dots, 10$ at all points $t = \tau, \dots, T$. As each value of $\lambda_i(t)$ reflects behaviour over the previous 90 days, the figure begins with July 2020. Lighter values indicate greater values of $d^{10}(s, t)$.

following the primary change point in March/April 2021.

5. Vaccine rollout consistency

In this section, we study the collective consistency between countries' vaccine rollouts and economic indicators such as their gross domestic product (GDP) and human development index (HDI). To do so, we introduce the following variables. Let $v_i(t)$ be the multivariate time series that records the fully vaccinated percentage of a country's population over time, $i = 1, \dots, N$ and $t = 1, \dots, T$. Our country-specific GDP and HDI scores are indexed g_i and h_i respectively, $i = 1, \dots, N$. As we wish to restrict attention to the period of global vaccine proliferation, this section restricts analysis from 1 February 2021 to 1 May 2022, a period of $T = 455$ days. For purposes of illustration, we plot the trajectory of $v_i(t)$ for select countries in Figure 5. To explore the time-varying consistency between countries' vaccination rollout and their GDP and HDI, we proceed as follows. At each time t , we construct the following distance matrices:

$$D_{ij}^{GDP} = |g_i - g_j|; \quad (10)$$

$$D_{ij}^{HDI} = |h_i - h_j|; \quad (11)$$

$$D(t)_{ij}^V = |v_i(t) - v_j(t)|. \quad (12)$$

We then convert each distance matrix into an *affinity matrix* using the same definition as (5):

$$A_{ij}^{GDP} = 1 - \frac{D_{ij}^{GDP}}{\max\{D^{GDP}\}}; \quad (13)$$

$$A_{ij}^{HDI} = 1 - \frac{D_{ij}^{HDI}}{\max\{D^{HDI}\}}; \quad (14)$$

$$A_{ij}^V(t) = 1 - \frac{D_{ij}^V(t)}{\max\{D^V(t)\}}, i, j = 1, \dots, N, t = 1, \dots, T. \quad (15)$$

$$(16)$$

These affinity matrices are appropriately normalised and can be compared directly to study the consistency between vaccine proliferation and HDI/GDP. We generate two *inconsistency matrices* as follows:

$$\text{INC}^{HDI,V}(t) = A^V(t) - A^{HDI}; \quad (17)$$

$$\text{INC}^{GDP,V}(t) = A^V(t) - A^{GDP}. \quad (18)$$

A larger absolute value of an entry in the matrix $\text{INC}^{HDI,V}(t)$ indicates that the relationships between two countries regarding HDI and their vaccination percentage at a point in time are quite different, analogously for $\text{INC}^{GDP,V}(t)$. To explore the collective consistency between such attributes across our entire collection, we calculate the L^1 norm of our resulting consistency matrices and

study how they evolve over time. For a $N \times N$ matrix A , its L^1 norm is defined by $\|A\| = \sum_{i,j=1}^N |A_{ij}|$. We compute the following sequence of matrix norms:

$$\nu_{HDI,V}^{INC}(t) = \|INC^{HDI,V}(t)\|; \quad (19)$$

$$\nu_{GDP,V}^{INC}(t) = \|INC^{GDP,V}(t)\|. \quad (20)$$

In Figure 6, we display both $\nu_{HDI,V}^{INC}(t)$ and $\nu_{GDP,V}^{INC}(t)$ as a function of time. These curves allow one to identify points in time where levels of economic and human development are most strongly associated with the proportion of the population that is fully vaccinated. This is marked by the time where both functions are minimal, namely where there is the least inconsistency (or greatest consistency) between economic/human development and country vaccine proliferation.

It is notable throughout our period of analysis that both consistency norm functions share a similar evolution, with both curves exhibiting a concave-up shape. That is, both inconsistency matrices start with relatively high inconsistencies, decrease during the initial stage of our analysis, and ultimately revert to their initial consistency. These two curves reveal several findings of interest. First, the broadly similar trajectories of the two curves indicate that GDP and HDI are broadly similar in their time-varying association with vaccine proliferation. They share the same down-up paths and global minima at very similar dates. Second, given that the HDI/vaccine inconsistency norm function reaches a lower point than the GDP/vaccine inconsistency norm, one could argue that HDI is more closely associated with vaccine rollout speed than GDP. Third, there is an interesting plausible explanation for the concave-up shape of each trajectory. Initially, when very few countries had administered their COVID-19 vaccination program, large discrepancies between GDP/HDI and vaccination rollout come from natural variability between countries' level of economic and human development. The point at which both inconsistency norm functions are lowest, which indicates the greatest level of consistency, can be explained by the more developed countries having mostly completed their vaccination programs. By the end of our window of analysis, when inconsistency matrix norms return close to their original values, less developed countries had begun to administer their COVID-19 vaccination program, and inconsistencies are driven by natural variation between countries' GDP and HDI values.

More broadly, this method of analysis could be used for exploring time-varying consistency between such attributes at a finer level. For example, one could subset two distinct collections of developed vs developing countries and analyse the extent of consistency between HDI/GDP and vaccine proliferation within each subsetted group.

6. Community-level vaccine effectiveness

In this section, we investigate broad trends in the association between the global vaccine rollout and case/death counts on a country-by-country basis.

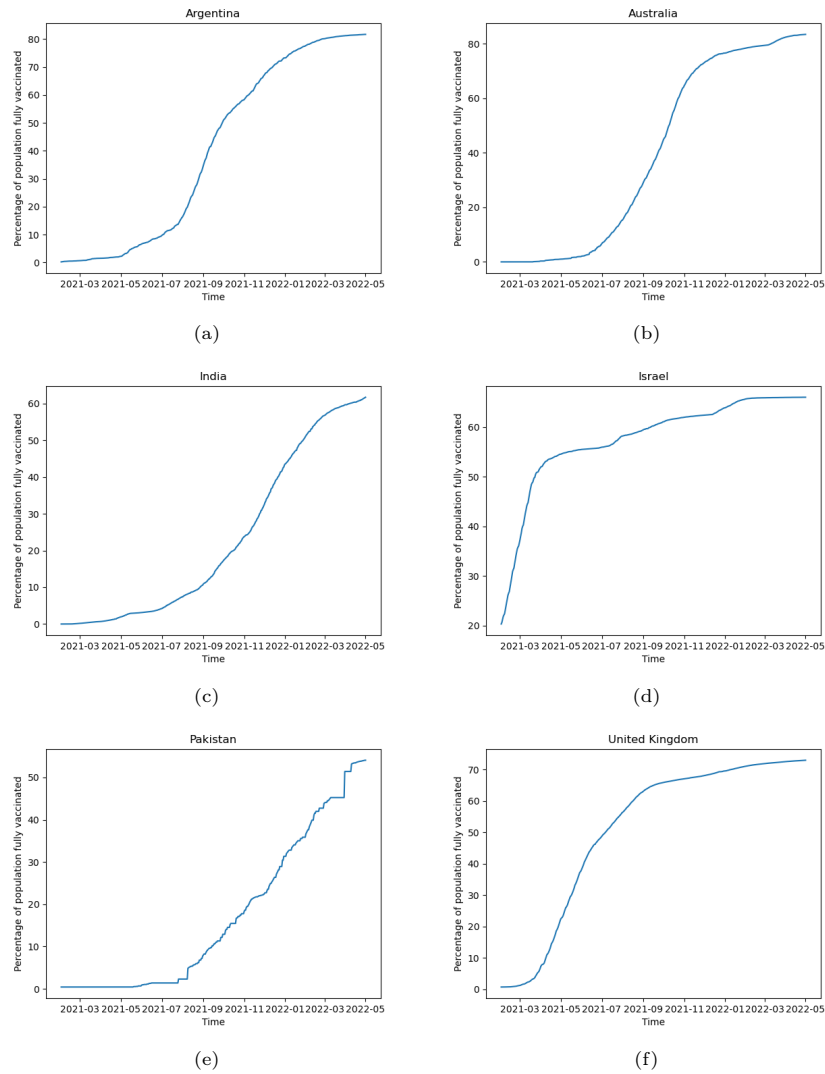


Figure 5: Time-varying rate of the population that is fully vaccinated for (a) Argentina, (b) Australia, (c) India, (d) Israel, (e) Pakistan and (f) the United Kingdom. Countries that were more efficient in fully vaccinating their population, such as Israel, have a steeper gradient, at an earlier point in time. Countries that were less efficient, such as Pakistan, have a less steep gradient commencing at a later point in our analysis window.

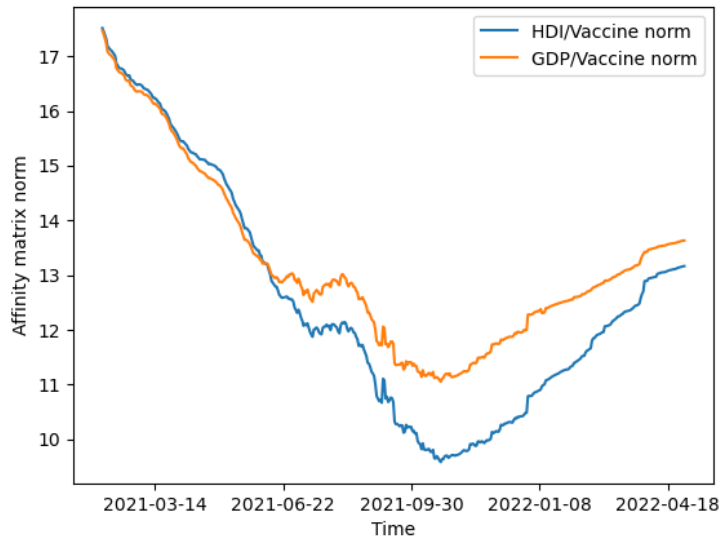


Figure 6: Time-varying collective consistency between vaccine proliferation and economic/human development, as defined in (19) and (20). There are several points of interest in the graph. First, both functions share a very similar evolution. Second, we see a global minimum at near-identical points, reflecting the similar association between vaccine proliferation and either HDI or GDP. Finally, the fact that HDI/vaccine consistency is regularly lower than GDP/vaccine consistency suggests that there is greater consistency between countries' human development index and the speed and progress of their vaccine rollout.

Mirroring the notation of Section 3, let $x_i(t), y_i(t)$ be the multivariate time series of new daily COVID-19 cases and deaths, respectively, in each of the N countries, $i = 1, \dots, N$ and $t = 1, \dots, T$. We perform two regression experiments to gain insight into the relationship between case and death counts with time and the rollout of vaccines.

We define a new quantity of interest,

$$W(t) = \frac{1}{t} \int_{s=1}^t v(s) ds = \frac{1}{t} \sum_{s=1}^t v(s). \quad (21)$$

We term this the *community vaccine integral*. This is a measure not just of the current level of vaccine proliferation, but takes into account the accumulation of immunity in the population due to sustained and established immunity.

First, we consider a simple linear regression model:

$$\log(x_i(t)) = \beta_0^X + \beta_1^X W(t) + \epsilon(t); \quad (22)$$

$$\log(y_i(t)) = \beta_0^Y + \beta_1^Y W(t) + \epsilon(t). \quad (23)$$

between the cases and deaths (in logarithmic space), respectively and this accumulation of immunity $W(t)$. Each country yields a value of β_1^X and β_1^Y reflective of the “best fit” (according to ordinary least squares [101, 102]) of the relationship between cases/deaths and $W(t)$. Applying the logarithm prior to fitting the regression can benefit in circumstances where cases (or any other quantity) can vary substantially in order of magnitude [103, 104]. In Table 1, we record the mean and variance of all values β_1 across all countries (for both cases and deaths). There are marked differences in coefficient behaviours across the two models. There is a strongly negative relationship between the community vaccine integral and deaths, demonstrating that greater accumulation of fully vaccinated individuals within a country is associated with reduced COVID-19 related deaths. The mean coefficient across our 50 countries is -1.17. The cases model has a considerably different relationship between the two variables. The average β_1 coefficient when studying log cases as the response variable is 0.89. This suggests that the accumulation of fully vaccinated individuals in various country communities had no effect in reducing COVID-19 cases. It is worth noting that the variance in coefficient estimates (among both models) were highly similar, with the log cases and log deaths models exhibiting variances among the β_1 ’s of 8.5 and 8.41, respectively.

We remark that by definition, the quantity $W(t)$ is monotonically non-decreasing with time, as $v(t)$ itself is. Thus, it possesses a close relationship with the variable t itself. To elucidate the relationship between cases/deaths, accumulation of immunity and time, we employ a random forest model, focusing on the feature importance of both time and $W(t)$.

Specifically, for each individual country, we employ a random forest model to analyse the relationship between $\log(x_i(t))$ (and analogously $\log(y_i(t))$) and

Linear regression coefficient mean and variance		
Response variable	Coefficient mean	Coefficient variance
log cases	0.89	8.5
log deaths	-1.17	8.41

Table 1: Mean and variance of linear regression β_1 coefficients over all 50 countries, for both the cases and deaths models, as defined in Section 6.

Random forest feature importance		
Response variable	Time	Vaccine integral
log cases	0.501	0.499
log deaths	0.504	0.496

Table 2: Mean feature importance from random forest model on log cases and log deaths of each country, as defined in Section 6.

both $W(t)$ and t simultaneously. This is typically notated as

$$\log(x_i(t)) \sim W(t), t. \quad (24)$$

In Table 2, we record the *feature importance* [102] of both $W(t)$ and t . This quantifies whether patterns in the case and death counts are more influenced by the accumulation of vaccination or the passage of time itself. The findings here are quite surprising. In both models, we see a highly similar relationship between the accumulation of full vaccination, time vs cases and deaths (our response variables). When we examine log cases as our response variable, time and vaccine accumulation yield feature importance scores of 0.501 and 0.499 respectively. Similarly, when we explore the impact these features have on log deaths, feature importance scores are 0.504 and 0.496, respectively. Beyond the fact that both variables may provide a similar level of explanatory power when determining variability in countries' cases and deaths, as both variables (other explicitly or implicitly) capture a temporal component, it is possible that this causes overlap in each feature's correlation with the response variable.

As a technical remark, these results were robust with numerous variations of parameters in implementing the random forest procedure. Prior to implementing both procedures, any case or death count of zero was adjusted to 1, so that the logarithm would be well defined.

7. Conclusion

In Section 3, we explore the time-varying infectivity of the COVID-19 pandemic, from its inception until current day. To do so, we implement time-varying principal components analysis and study the evolution of the strength of the correlation matrix's first eigenvalue. Our analysis identifies a period corresponding to early 2021, where we see an abrupt translation upward in the collective

strength of infectivity dynamics among the countries we have studied. The second key finding is the identification of periodic (oscillatory) trends in collective infectivity dynamics. Our assertion is that this periodic behaviour is driven by two key phenomena: the emergence of more infectious strains of COVID-19 (such as the Delta variant), and the “stop-start” nature of various countries’ economic reopenings.

In Section 4, we introduce a novel graph-theoretic framework to investigate and quantify the location of the change point identified in Section 3. Our graph theoretic framework confirms that this transition occurs in March/April 2021. We then introduce two matrices $d(s, t)$ and $d^{10}(s, t)$ that explore the evolutionary similarity in the eigenspectrum of the infectivity correlation matrix. Both matrices present findings that are broadly consistent, with the emergence of two noticeably concentrated sub-matrices which display limited affinity between the two.

In Section 5, we study the time-varying consistency between countries’ economic and human development (represented by HDI and GDP) against their COVID-19 vaccine rollout. To do so, we construct a variety of temporally-dependent affinity matrices, and explore the evolution of collective consistency. Our analysis confirms that our collection of countries shares a similar evolution in consistency between HDI and GDP with their respective accumulation of fully vaccinated individuals. Both trajectories share a global minimum that is virtually identical, which is indicative of a point in time where more developed countries displayed greater efficiency in their vaccine rollout. Finally, due to a higher level of consistency throughout our period of analysis, one can conclude that there is greater consistency between countries economic development (HDI) and their vaccine proliferation when compared to their economic development (GDP) and their vaccine proliferation.

In Section 6, we explicitly study the relationship between countries’ accumulation of fully vaccinated individuals and COVID-19 cases and deaths. To do so, we implement two supervised learning techniques (linear regression and random forest) and study the distribution of coefficient values and feature importance, for our cases and deaths models respectively. Our analysis reveals that there is a significantly negative relationship between a country’s vaccine accumulation and COVID-19 related deaths, while there is a positive (and significant) relationship with COVID-19 cases. One may conclude that the COVID-19 vaccine was highly effective in reducing deaths, but ineffective in stopping the spread of cases. The study of feature importance scores in our random forest implementation demonstrates that our vaccine accumulation metric and the passage of time itself are similarly important in both our cases and deaths models.

We are unaware of any work in the nonlinear dynamics community that takes a holistic approach to studying vaccine dynamics and their interplay with human/economic development indicators using techniques from a broad range of areas including nonlinear dynamics, graph theory and machine learning. In this work, we apply such methods to study a range of factors surrounding the pandemic including global infectivity, vaccine proliferation, economic and human development. Further work exploring the interplay between the vaccine and

other important factors would be welcomed by the community. Such analysis could help us better understand epidemiological dynamics during pandemics, and allow policymakers to implement better, data-driven decisions for optimal outcomes in the future.

Data availability statement

All the data in this paper are obtained from Our World in Data (<https://ourworldindata.org/coronavirus>).

References

- [1] F. Zhou, et al., Clinical course and risk factors for mortality of adult inpatients with COVID-19 in Wuhan, China: a retrospective cohort study, *The Lancet* 395 (2020) 1054–1062. doi:10.1016/s0140-6736(20)30566-3.
- [2] S. A. Lauer, et al., The incubation period of Coronavirus disease 2019 (COVID-19) from publicly reported confirmed cases: Estimation and application, *Annals of Internal Medicine* 172 (2020) 577–582. doi:10.7326/m20-0504.
- [3] F. Jiang, L. Deng, L. Zhang, Y. Cai, C. W. Cheung, Z. Xia, Review of the clinical characteristics of Coronavirus Disease 2019 (COVID-19), *Journal of General Internal Medicine* 35 (2020) 1545–1549. doi:10.1007/s11606-020-05762-w.
- [4] Z. Y. Zu, M. D. Jiang, P. P. Xu, W. Chen, Q. Q. Ni, G. M. Lu, L. J. Zhang, Coronavirus disease 2019 (COVID-19): A perspective from China, *Radiology* (2020) 200490. doi:10.1148/radiol.2020200490.
- [5] S. Chen, J. Yang, W. Yang, C. Wang, T. Bärnighausen, COVID-19 control in China during mass population movements at new year, *The Lancet* 395 (2020) 764–766. doi:10.1016/s0140-6736(20)30421-9.
- [6] G. Wang, Y. Zhang, J. Zhao, J. Zhang, F. Jiang, Mitigate the effects of home confinement on children during the COVID-19 outbreak, *The Lancet* 395 (2020) 945–947. doi:10.1016/s0140-6736(20)30547-x.
- [7] P. Zhou, et al., A pneumonia outbreak associated with a new coronavirus of probable bat origin, *Nature* 579 (2020) 270–273. doi:10.1038/s41586-020-2012-7.
- [8] M. Wang, et al., Remdesivir and chloroquine effectively inhibit the recently emerged novel coronavirus (2019-nCoV) in vitro, *Cell Research* 30 (2020) 269–271. doi:10.1038/s41422-020-0282-0.
- [9] E. M. Bloch, Convalescent plasma to treat COVID-19, *Blood* 136 (2020) 654–655. doi:10.1182/blood.2020007714.

- [10] X. Xu, et al., Effective treatment of severe COVID-19 patients with tocilizumab, *Proceedings of the National Academy of Sciences* 117 (2020) 10970–10975. doi:10.1073/pnas.2005615117.
- [11] B. Cao, et al., A trial of Lopinavir-Ritonavir in adults hospitalized with severe Covid-19, *New England Journal of Medicine* 382 (2020) 1787–1799. doi:10.1056/nejmoa2001282.
- [12] L. Corey, J. R. Mascola, A. S. Fauci, F. S. Collins, A strategic approach to COVID-19 vaccine R&D, *Science* 368 (2020) 948–950. doi:10.1126/science.abc5312.
- [13] F. P. Polack, et al., Safety and efficacy of the BNT162b2 mRNA Covid-19 vaccine, *New England Journal of Medicine* 383 (2020) 2603–2615. doi:10.1056/nejmoa2034577.
- [14] E. E. Walsh, et al., Safety and immunogenicity of two RNA-based Covid-19 vaccine candidates, *New England Journal of Medicine* 383 (2020) 2439–2450. doi:10.1056/nejmoa2027906.
- [15] H. Le, B. A. Khan, S. Murtaza, A. A. Shah, The increase in suicide during the COVID-19 pandemic, *Psychiatric Annals* 50 (2020) 526–530. doi:10.3928/00485713-20201105-01.
- [16] A. John, J. Pirkis, D. Gunnell, L. Appleby, J. Morrissey, Trends in suicide during the Covid-19 pandemic, *BMJ* (2020) m4352. doi:10.1136/bmj.m4352.
- [17] L. A. Burke, A. M. Ryan, The complex relationship between cost and quality in US health care, *AMA Journal of Ethics* 16 (2014) 124–130. doi:10.1001/virtualmentor.2014.16.2.pfor1-1402.
- [18] L. Wynants, et al., Prediction models for diagnosis and prognosis of covid-19: systematic review and critical appraisal, *BMJ* (2020) m1328. doi:10.1136/bmj.m1328.
- [19] E. Estrada, COVID-19 and SARS-CoV-2. Modeling the present, looking at the future, *Physics Reports* 869 (2020) 1–51. doi:10.1016/j.physrep.2020.07.005.
- [20] N. S. Barlow, S. J. Weinstein, Accurate closed-form solution of the SIR epidemic model, *Physica D: Nonlinear Phenomena* 408 (2020) 132540. doi:10.1016/j.physd.2020.132540.
- [21] S. J. Weinstein, M. S. Holland, K. E. Rogers, N. S. Barlow, Analytic solution of the SEIR epidemic model via asymptotic approximant, *Physica D: Nonlinear Phenomena* 411 (2020) 132633. doi:10.1016/j.physd.2020.132633.

- [22] K. Y. Ng, M. M. Gui, COVID-19: Development of a robust mathematical model and simulation package with consideration for ageing population and time delay for control action and resusceptibility, *Physica D: Nonlinear Phenomena* 411 (2020) 132599. doi:10.1016/j.physd.2020.132599.
- [23] C. Vyasarayani, A. Chatterjee, New approximations, and policy implications, from a delayed dynamic model of a fast pandemic, *Physica D: Nonlinear Phenomena* 414 (2020) 132701. doi:10.1016/j.physd.2020.132701.
- [24] M. Cadoni, G. Gaeta, Size and timescale of epidemics in the SIR framework, *Physica D: Nonlinear Phenomena* 411 (2020) 132626. doi:10.1016/j.physd.2020.132626.
- [25] A. G. Neves, G. Guerrero, Predicting the evolution of the COVID-19 epidemic with the a-SIR model: Lombardy, Italy and São Paulo state, Brazil, *Physica D: Nonlinear Phenomena* 413 (2020) 132693. doi:10.1016/j.physd.2020.132693.
- [26] A. Comunian, R. Gaburro, M. Giudici, Inversion of a SIR-based model: A critical analysis about the application to COVID-19 epidemic, *Physica D: Nonlinear Phenomena* 413 (2020) 132674. doi:10.1016/j.physd.2020.132674.
- [27] T. Sun, Y. Wang, Modeling COVID-19 epidemic in Heilongjiang province, China, *Chaos, Solitons & Fractals* 138 (2020) 109949. doi:10.1016/j.chaos.2020.109949.
- [28] A. Ballesteros, A. Blasco, I. Gutierrez-Sagredo, Hamiltonian structure of compartmental epidemiological models, *Physica D: Nonlinear Phenomena* 413 (2020) 132656. doi:10.1016/j.physd.2020.132656.
- [29] S. Liu, M. Y. Li, Epidemic models with discrete state structures, *Physica D: Nonlinear Phenomena* 422 (2021) 132903. doi:10.1016/j.physd.2021.132903.
- [30] N. M. Gatto, H. Schellhorn, Optimal control of the SIR model in the presence of transmission and treatment uncertainty, *Mathematical Biosciences* 333 (2021) 108539. doi:10.1016/j.mbs.2021.108539.
- [31] C. Manchein, E. L. Brugnago, R. M. da Silva, C. F. O. Mendes, M. W. Beims, Strong correlations between power-law growth of COVID-19 in four continents and the inefficiency of soft quarantine strategies, *Chaos: An Interdisciplinary Journal of Nonlinear Science* 30 (2020) 041102. doi:10.1063/5.0009454.
- [32] B. Blasius, Power-law distribution in the number of confirmed COVID-19 cases, *Chaos: An Interdisciplinary Journal of Nonlinear Science* 30 (2020) 093123. doi:10.1063/5.0013031.

- [33] B. K. Beare, A. A. Toda, On the emergence of a power law in the distribution of COVID-19 cases, *Physica D: Nonlinear Phenomena* 412 (2020) 132649. doi:10.1016/j.physd.2020.132649.
- [34] M. Perc, N. G. Miksić, M. Slavinec, A. Stožer, Forecasting COVID-19, *Frontiers in Physics* 8 (2020) 127. doi:10.3389/fphy.2020.00127.
- [35] S. Boccaletti, W. Ditto, G. Mindlin, A. Atangana, Modeling and forecasting of epidemic spreading: The case of Covid-19 and beyond, *Chaos, Solitons & Fractals* 135 (2020) 109794. doi:10.1016/j.chaos.2020.109794.
- [36] O. Castillo, P. Melin, Forecasting of COVID-19 time series for countries in the world based on a hybrid approach combining the fractal dimension and fuzzy logic, *Chaos, Solitons & Fractals* 140 (2020) 110242. doi:10.1016/j.chaos.2020.110242.
- [37] O. Castillo, P. Melin, A novel method for a COVID-19 classification of countries based on an intelligent fuzzy fractal approach, *Healthcare* 9 (2021) 196. doi:10.3390/healthcare9020196.
- [38] P. Melin, J. C. Monica, D. Sanchez, O. Castillo, Multiple ensemble neural network models with fuzzy response aggregation for predicting COVID-19 time series: The case of Mexico, *Healthcare* 8 (2020) 181. doi:10.3390/healthcare8020181.
- [39] N. James, M. Menzies, Optimally adaptive Bayesian spectral density estimation for stationary and nonstationary processes, *Statistics and Computing* 32 (2022) 45. doi:10.1007/s11222-022-10103-4.
- [40] D. Manevski, N. R. Gorenjec, N. Kejžar, R. Blagus, Modeling COVID-19 pandemic using Bayesian analysis with application to Slovene data, *Mathematical Biosciences* 329 (2020) 108466. doi:10.1016/j.mbs.2020.108466.
- [41] N. James, M. Menzies, Trends in COVID-19 prevalence and mortality: A year in review, *Physica D: Nonlinear Phenomena* 425 (2021) 132968. doi:10.1016/j.physd.2021.132968.
- [42] K. Shang, B. Yang, J. M. Moore, Q. Ji, M. Small, Growing networks with communities: A distributive link model, *Chaos: An Interdisciplinary Journal of Nonlinear Science* 30 (2020) 041101. doi:10.1063/5.0007422.
- [43] A. Karaivanov, A social network model of COVID-19, *PLOS ONE* 15 (2020) e0240878. doi:10.1371/journal.pone.0240878.
- [44] J. Ge, D. He, Z. Lin, H. Zhu, Z. Zhuang, Four-tier response system and spatial propagation of COVID-19 in China by a network model, *Mathematical Biosciences* 330 (2020) 108484. doi:10.1016/j.mbs.2020.108484.

- [45] L. Xue, S. Jing, J. C. Miller, W. Sun, H. Li, J. G. Estrada-Franco, J. M. Hyman, H. Zhu, A data-driven network model for the emerging COVID-19 epidemics in Wuhan, Toronto and Italy, *Mathematical Biosciences* 326 (2020) 108391. doi:10.1016/j.mbs.2020.108391.
- [46] F. Saldaña, H. Flores-Arguedas, J. A. Camacho-Gutiérrez, I. B. and, Modeling the transmission dynamics and the impact of the control interventions for the COVID-19 epidemic outbreak, *Mathematical Biosciences and Engineering* 17 (2020) 4165–4183. doi:10.3934/mbe.2020231.
- [47] A. Danchin, G. Turinici, Immunity after COVID-19: Protection or sensitization?, *Mathematical Biosciences* 331 (2021) 108499. doi:10.1016/j.mbs.2020.108499.
- [48] N. James, M. Menzies, Cluster-based dual evolution for multivariate time series: Analyzing COVID-19, *Chaos: An Interdisciplinary Journal of Nonlinear Science* 30 (2020) 061108. doi:10.1063/5.0013156.
- [49] J. A. T. Machado, A. M. Lopes, Rare and extreme events: the case of COVID-19 pandemic, *Nonlinear Dynamics* (2020). doi:10.1007/s11071-020-05680-w.
- [50] N. James, M. Menzies, P. Radchenko, COVID-19 second wave mortality in Europe and the United States, *Chaos: An Interdisciplinary Journal of Nonlinear Science* 31 (2021) 031105. doi:10.1063/5.0041569.
- [51] C. N. Ngonghala, E. A. Iboi, A. B. Gumel, Could masks curtail the post-lockdown resurgence of COVID-19 in the US?, *Mathematical Biosciences* 329 (2020) 108452. doi:10.1016/j.mbs.2020.108452.
- [52] J. Cavataio, S. Schnell, Interpreting SARS-CoV-2 seroprevalence, deaths, and fatality rate — making a case for standardized reporting to improve communication, *Mathematical Biosciences* 333 (2021) 108545. doi:10.1016/j.mbs.2021.108545.
- [53] N. James, M. Menzies, Estimating a continuously varying offset between multivariate time series with application to COVID-19 in the United States, *The European Physical Journal Special Topics* (2022). doi:10.1140/epjs/s11734-022-00430-y.
- [54] L. Ó. Náraigh, Á. Byrne, Piecewise-constant optimal control strategies for controlling the outbreak of COVID-19 in the Irish population, *Mathematical Biosciences* 330 (2020) 108496. doi:10.1016/j.mbs.2020.108496.
- [55] D. H. Glass, European and US lockdowns and second waves during the COVID-19 pandemic, *Mathematical Biosciences* 330 (2020) 108472. doi:10.1016/j.mbs.2020.108472.

- [56] M. Akhtaruzzaman, S. Boubaker, A. Sensoy, Financial contagion during COVID–19 crisis, *Finance Research Letters* (2020) 101604. doi:10.1016/j.fr1.2020.101604.
- [57] M. Akhtaruzzaman, S. Boubaker, B. M. Lucey, A. Sensoy, Is gold a hedge or safe haven asset during COVID–19 crisis?, *SSRN Electronic Journal* (2020). doi:10.2139/ssrn.3621358.
- [58] N. James, M. Menzies, Association between COVID-19 cases and international equity indices, *Physica D: Nonlinear Phenomena* 417 (2021) 132809. doi:10.1016/j.physd.2020.132809.
- [59] A. Zaremba, R. Kizys, D. Y. Aharon, E. Demir, Infected markets: Novel coronavirus, government interventions, and stock return volatility around the globe, *Finance Research Letters* 35 (2020) 101597. doi:10.1016/j.fr1.2020.101597.
- [60] D. I. Okorie, B. Lin, Stock markets and the COVID-19 fractal contagion effects, *Finance Research Letters* (2020) 101640. doi:10.1016/j.fr1.2020.101640.
- [61] N. James, M. Menzies, J. Chan, Changes to the extreme and erratic behaviour of cryptocurrencies during COVID-19, *Physica A: Statistical Mechanics and its Applications* 565 (2021) 125581. doi:10.1016/j.physa.2020.125581.
- [62] S. Lahmiri, S. Bekiros, The impact of COVID-19 pandemic upon stability and sequential irregularity of equity and cryptocurrency markets, *Chaos, Solitons & Fractals* 138 (2020) 109936. doi:10.1016/j.chaos.2020.109936.
- [63] N. James, M. Menzies, Collective correlations, dynamics, and behavioural inconsistencies of the cryptocurrency market over time, *Nonlinear Dynamics* 107 (2022) 4001–4017. doi:10.1007/s11071-021-07166-9.
- [64] E. Mnif, A. Jarboui, K. Mouakhar, How the cryptocurrency market has performed during COVID 19? A multifractal analysis, *Finance Research Letters* 36 (2020) 101647. doi:10.1016/j.fr1.2020.101647.
- [65] N. James, M. Menzies, Efficiency of communities and financial markets during the 2020 pandemic, *Chaos: An Interdisciplinary Journal of Nonlinear Science* 31 (2021) 083116. doi:10.1063/5.0054493.
- [66] J. W. Goodell, S. Goutte, Co-movement of COVID-19 and Bitcoin: Evidence from wavelet coherence analysis, *Finance Research Letters* (2020) 101625. doi:10.1016/j.fr1.2020.101625.
- [67] N. James, Dynamics, behaviours, and anomaly persistence in cryptocurrencies and equities surrounding COVID-19, *Physica A: Statistical Mechanics and its Applications* 570 (2021) 125831. doi:10.1016/j.physa.2021.125831.

- [68] M. B. Arouxet, A. F. Bariviera, V. E. Pastor, V. Vampa, Covid-19 impact on cryptocurrencies: evidence from a wavelet-based Hurst exponent, 2020. [arXiv:2009.05652](https://arxiv.org/abs/2009.05652).
- [69] N. James, K. Chin, On the systemic nature of global inflation, its association with equity markets and financial portfolio implications, *Physica A: Statistical Mechanics and its Applications* 593 (2022) 126895. doi:10.1016/j.physa.2022.126895.
- [70] Y. Zhou, et al., A spatiotemporal epidemiological prediction model to inform county-level COVID-19 risk in the United States, *Harvard Data Science Review* (2020). doi:10.1162/99608f92.79e1f45e.
- [71] P. Melin, J. C. Monica, D. Sanchez, O. Castillo, Analysis of spatial spread relationships of coronavirus (COVID-19) pandemic in the world using self organizing maps, *Chaos, Solitons & Fractals* 138 (2020) 109917. doi:10.1016/j.chaos.2020.109917.
- [72] N. James, M. Menzies, H. Bondell, Understanding spatial propagation using metric geometry with application to the spread of COVID-19 in the United States, *EPL (Europhysics Letters)* 135 (2021) 48004. doi:10.1209/0295-5075/ac2752.
- [73] Y. Wang, Y. Liu, J. Struthers, M. Lian, Spatiotemporal characteristics of the COVID-19 epidemic in the United States, *Clinical Infectious Diseases* 72 (2020) 643–651. doi:10.1093/cid/ciaa934.
- [74] N. James, M. Menzies, H. Bondell, Comparing the dynamics of COVID-19 infection and mortality in the United States, India, and Brazil, *Physica D: Nonlinear Phenomena* 432 (2022) 133158. doi:10.1016/j.physd.2022.133158.
- [75] V. Priesemann, R. Balling, M. M. Brinkmann, S. Ciesek, T. Czypionka, I. Eckerle, G. Giordano, C. Hanson, Z. Hel, P. Hotulainen, P. Klimek, A. Nassehi, A. Peichl, M. Perc, E. Petelos, B. Prainsack, E. Szczurek, An action plan for pan-european defence against new SARS-CoV-2 variants, *The Lancet* 397 (2021) 469–470. doi:10.1016/s0140-6736(21)00150-1.
- [76] V. Priesemann, R. Balling, S. Bauer, P. Beutels, A. C. Valdez, S. Cuschieri, T. Czypionka, U. Dumpis, E. Glaab, E. Grill, P. Hotulainen, E. N. Iftekhhar, J. Krutzinna, C. Lionis, H. Machado, C. Martins, M. McKee, G. N. Pavlakis, M. Perc, E. Petelos, M. Pickersgill, B. Prainsack, J. Rocklöv, E. Schernhammer, E. Szczurek, S. Tsiodras, S. V. Gucht, P. Willeit, Towards a european strategy to address the COVID-19 pandemic, *The Lancet* (2021). doi:10.1016/s0140-6736(21)01808-0.
- [77] M. Piraveenan, S. Sawleshwarkar, M. Walsh, I. Zablotska, S. Bhattacharyya, H. H. Farooqui, T. Bhatnagar, A. Karan, M. Murhekar, S. Zodpey, K. S. M.

- Rao, P. Pattison, A. Zomaya, M. Perc, Optimal governance and implementation of vaccination programmes to contain the COVID-19 pandemic, *Royal Society Open Science* 8 (2021) 210429. doi:10.1098/rsos.210429.
- [78] K. J. Spensley, S. Gleeson, P. Martin, T. Thomson, C. L. Clarke, G. Pickard, D. Thomas, S. P. McAdoo, P. Randell, P. Kelleher, R. Bedi, L. Lightstone, M. Prendecki, M. Willicombe, Comparison of vaccine effectiveness against the Omicron (B.1.1.529) variant in hemodialysis patients, *Kidney International Reports* 7 (2022) 1406–1409. doi:10.1016/j.ekir.2022.04.005.
- [79] J. S. Tregoning, K. E. Flight, S. L. Higham, Z. Wang, B. F. Pierce, Progress of the COVID-19 vaccine effort: viruses, vaccines and variants versus efficacy, effectiveness and escape, *Nature Reviews Immunology* 21 (2021) 626–636. doi:10.1038/s41577-021-00592-1.
- [80] A. M. Lisewski, Effectiveness of England’s initial vaccine roll out, *BMJ* (2021) n1201. doi:10.1136/bmj.n1201.
- [81] S. K. Sharma, A. Bangia, M. Alshehri, R. Bhardwaj, Nonlinear dynamics for the spread of pathogenesis of COVID-19 pandemic, *Journal of Infection and Public Health* 14 (2021) 817–831. doi:10.1016/j.jiph.2021.04.001.
- [82] N. James, M. Menzies, COVID-19 in the United States: Trajectories and second surge behavior, *Chaos: An Interdisciplinary Journal of Nonlinear Science* 30 (2020) 091102. doi:10.1063/5.0024204.
- [83] P. Gopikrishnan, B. Rosenow, V. Plerou, H. E. Stanley, Quantifying and interpreting collective behavior in financial markets, *Physical Review E* 64 (2001). doi:10.1103/physreve.64.035106.
- [84] A. Prakash, N. James, M. Menzies, G. Francis, Structural clustering of volatility regimes for dynamic trading strategies, *Applied Mathematical Finance* 28 (2021) 236–274. doi:10.1080/1350486x.2021.2007146.
- [85] L. Laloux, P. Cizeau, J.-P. Bouchaud, M. Potters, Noise dressing of financial correlation matrices, *Physical Review Letters* 83 (1999) 1467–1470. doi:10.1103/physrevlett.83.1467.
- [86] N. James, M. Menzies, A new measure between sets of probability distributions with applications to erratic financial behavior, *Journal of Statistical Mechanics: Theory and Experiment* 2021 (2021) 123404. doi:10.1088/1742-5468/ac3d91.
- [87] V. Plerou, P. Gopikrishnan, B. Rosenow, L. A. N. Amaral, T. Guhr, H. E. Stanley, Random matrix approach to cross correlations in financial data, *Physical Review E* 65 (2002). doi:10.1103/physreve.65.066126.
- [88] F. Arroyo-Marioli, F. Bullano, S. Kucinskas, C. Rondón-Moreno, Tracking R of COVID-19: A new real-time estimation using the Kalman filter, *PLOS ONE* 16 (2021) e0244474. doi:10.1371/journal.pone.0244474.

- [89] D. J. Fenn, M. A. Porter, S. Williams, M. McDonald, N. F. Johnson, N. S. Jones, Temporal evolution of financial-market correlations, *Physical Review E* 84 (2011). doi:10.1103/physreve.84.026109.
- [90] N. James, M. Menzies, G. A. Gottwald, On financial market correlation structures and diversification benefits across and within equity sectors, *Physica A: Statistical Mechanics and its Applications* (2022) 127682. doi:10.1016/j.physa.2022.127682.
- [91] A. J. Heckens, S. M. Krause, T. Guhr, Uncovering the dynamics of correlation structures relative to the collective market motion, *Journal of Statistical Mechanics: Theory and Experiment* 2020 (2020) 103402. doi:10.1088/1742-5468/abb6e2.
- [92] N. James, M. Menzies, J. Chan, Semi-metric portfolio optimization: a new algorithm reducing simultaneous asset shocks, 2021. doi:10.48550/arXiv.2001.09404.
- [93] R. K. Pan, S. Sinha, Collective behavior of stock price movements in an emerging market, *Physical Review E* 76 (2007). doi:10.1103/physreve.76.046116.
- [94] D. Wilcox, T. Gebbie, An analysis of cross-correlations in an emerging market, *Physica A: Statistical Mechanics and its Applications* 375 (2007) 584–598. doi:10.1016/j.physa.2006.10.030.
- [95] N. James, M. Menzies, K. Chin, Economic state classification and portfolio optimisation with application to stagflationary environments, 2022. doi:10.48550/arXiv.2203.15911.
- [96] W. Rudin, *Functional Analysis*, McGraw-Hill Science, 1991.
- [97] J. H. Ward, Hierarchical grouping to optimize an objective function, *Journal of the American Statistical Association* 58 (1963) 236–244. doi:10.1080/01621459.1963.10500845.
- [98] G. J. Szekely, M. L. Rizzo, Hierarchical clustering via joint between-within distances: Extending Ward’s minimum variance method, *Journal of Classification* 22 (2005) 151–183. doi:10.1007/s00357-005-0012-9.
- [99] N. James, M. Menzies, L. Azizi, J. Chan, Novel semi-metrics for multivariate change point analysis and anomaly detection, *Physica D: Nonlinear Phenomena* 412 (2020) 132636. doi:10.1016/j.physd.2020.132636.
- [100] D. Müllner, Fastcluster: Fast hierarchical, agglomerative clustering routines for RandPython, *Journal of Statistical Software* 53 (2013). doi:10.18637/jss.v053.i09.
- [101] N. James, M. Menzies, H. Bondell, In search of peak human athletic potential: a mathematical investigation, *Chaos: An Interdisciplinary Journal of Nonlinear Science* 32 (2022) 023110. doi:10.1063/5.0073141.

- [102] T. Hastie, R. Tibshirani, J. Friedman, *The Elements of Statistical Learning*, Springer New York, 2009. doi:10.1007/978-0-387-84858-7.
- [103] N. James, M. Menzies, Spatio-temporal trends in the propagation and capacity of low-carbon hydrogen projects, *International Journal of Hydrogen Energy* 47 (2022) 16775–16784. doi:10.1016/j.ijhydene.2022.03.198.
- [104] G. James, D. Witten, T. Hastie, R. Tibshirani, *An Introduction to Statistical Learning*, Springer, 2013.